IEEE Access
Multidisciplinary | Rapid Review | Open Access Journal

Received December 31, 2019, accepted January 13, 2020, date of publication January 20, 2020, date of current version January 31, 2020.

Digital Object Identifier 10.1109/ACCESS.2020.2968086

Novel Methods for Modeling and Online Measurement of Effective Bulk Modulus of Flowing Oil

BAOLONG GENG, LICHEN GU, AND JIAMIN LIU
Institute of Electromechanical Technology, Xi'an University of Architecture and Technology, Xi'an 710064, China
Corresponding author: Lichen Gu (gulichen@ 126.com)

This work was supported by the National Natural Science Foundation of China under Grant 51675399.

ABSTRACT Oil is a key medium for transmitting power and coupling information in the hydraulic transmission system. Accurate calculation and measurement of the dynamic compressibility of the oil have profound significance to the system performance analysis. The present study primarily focuses on the effect of steady pressure on the bulk modulus of static oil. However, changing pressure and flowing oil are the general working conditions in most of hydraulic apparatus. There are few researchers paying attention to the influence of pressure on the compressibility of flowing oil. Considering the log-normal distribution of bubble size in oil, an improved static oil model (Model B) is developed to calculate the bulk modulus of the motionless oil under the dynamic pressure. Then, by deriving Model B, this paper proposes an original flowing oil model (Model C) to determine the effective bulk modulus of flowing oil. Finally, based on the inherent pressure pulsation of the axial piston pump, an innovative online method for measurement of the bulk modulus of flowing oil is presented as it has the advantage of avoiding interference with flow stability. It has been proved that the changes in the flow velocity corresponds to the crucial effect on the effective bulk modulus of flowing oil, especially under the low-flow and low-pressure operation conditions. Those results and analysis provide promoting support for identifying and determining the effective bulk modulus of oil, analyzing the system stiffness, improving the control accuracy, as well as optimizing the mathematical models.

INDEX TERMS Bulk modulus, bubble size distribution, flowing oil, online measurement.

I. INTRODUCTION

Hydraulic driving and controlling technologies are generally adopted in different walks of life, such as engineering construction, metallurgy, mining, national defense and materials. The oil acts as a crucial medium for the energy transmission and information coupling in the hydraulic transmission system, where its compressibility affects the stiffness [1]–[3], control accuracy [4], [5], dynamic and the nonlinear performance [6]–[9] of the system. Moreover, in the fields such as fault diagnosis [10], [11], condition monitoring [12], and reliability research, without paying attention to the nonstationary compressibility of the oil would cause misjudgment of the system running state.

The associate editor coordinating the review of this manuscript and approving it for publication was Tao Wang.

The bulk modulus of oil is nonstationary and susceptible to the disturbance in the system. It has been proved that the nonlinear variation of the bulk modulus is mainly caused by the undissolved bubbles in the liquid [13]. During the operation, free air can be mixed into the hydraulic fluid in multiple ways, including air drawn into oil through the leakage of the pipeline or the accumulators, oil exposed in air, and even the dissolved air separated from the oil under low-pressure condition. All of those aforementioned factors produce bubbles [14], [15]. The low-density and the large molecular gap of bubbles bring in large volume change under the varying pressure, and affects the compressibility of the liquid.

The increase of air content causes great deformation and increases the nonlinearity of bulk modulus of the liquid [16]. Many studies have attempted to reduce the air content by degassing for a better compressibility [6], [17], [18].

However, it is conventionally not available due to its cost consideration, environment/space limitations and inefficiency.

The traditional models for bulk modulus assumed that the air content is constant [18], [19]. They considered the bulk modulus of oil as pressure-dependent and did not take into account the dissolved air. IFSA and AMEsim modified the traditional models base on the Henry's law [15]. However, the limitation of those modified models is that it is unable to capture the dynamic air absorption or release.

Some studies [16], [20], [21] pointed out that the dynamic transfer of mass between bubbles and oil are non-equilibrium during compression in most cases. Oil in liquid takes much longer to reach equilibrium by compression than by pressure release. Therefore, to understand the real-time bulk modulus of oil, the dynamic of absorption or release of the air under the non-equilibrium state should be considered. Schmitz and Murrenhoff [15] estimated the time of entire dissolution by experiment. They assumed the air dissolution rate to be uniform within a certain time for calculating the real-time bulk modulus of oil. Zhou *et al.* [22] determined the time of inter-phase mass transfer by the Rayleigh-Plesset equation. Tian and Van de Ven [14] simplified the physical meaning of the mass transfer coefficient, and pointed out the dissolving rate of air is affected by the size of bubble.

In reviewing the literature, the majority of scholars mainly focused on the effect of steady pressure on the dynamic transfer of mass between the free air and the oil. There are few studies paying attention to the compressibility of flowing oil. In reality, the flowing oil and the variable pressure are the typical style in hydraulic apparatuses. Introducing the bulk modulus of the static oil into the flowing oil with a simple manner would cause errors. This paper will focus on analyzing the compressibility of static oil under the variable operation conditions, and discussing the association of the flow and the pressure with the effective bulk modulus of flowing oil.

The main contributions of this paper are listed as follows:

- By introducing the log-normal distribution of bubble size and deriving the mass transfer differential equation(Model A), we propose an improved static oil model(Model B) to determine the bulk modulus of the static oil under variable pressure conditions. It has a great effect in improving the calculation accuracy of the static oil bulk modulus and extending the application of the static oil model under the variable pressure conditions.
- On the premise of the laminar flow in the pipeline, an original flowing oil model(Model C) based on the improved static oil model is developed to determine the effective bulk modulus of flowing oil.
- Based on the inherent pressure pulsation of the axial piston pump, an innovative online measuring method of the bulk modulus of the flowing oil is introduced, which has the advantage of avoiding interference with flow stability during the online measurement.
- The simulation and experimental results prove that the varying in flow rate corresponds to the changes of effective bulk modulus of the flowing oil in the pipeline, especially under low-flow and low-pressure operation conditions.

The rest of this paper is organized as follows. The principle and implementation of the bulk modulus models of static oil and the flowing oil are elaborated in Section II. The third section presents an experiment to verify the models in Section II. The fourth section is the discussion of some results of extended research on those models. Conclusions are given in the fifth Section.

II. THEORETICAL DEVELOPMENT

A. CALCULATION OF THE EFFECTIVE BULK MODULUS

According to the definition, the tangential bulk moduli of air K_g, pure oil K_o, and mixed liquid K_e are calculated as follows, respectively.

$$K_g = -V_g \frac{dP}{dV_g} \tag{1}$$

$$K_o = -V_o \frac{dP}{dV_o} \tag{2}$$

$$K_e = -(V_o + V_g) \frac{dP}{dV_o + dV_g} \tag{3}$$

Substituting Eq. (1) and Eq. (2) into Eq. (3), and further simplify it, the expression of K_e is given as follows:

$$K_e = \frac{V_o + V_g}{\frac{V_g}{K_g} + \frac{V_o}{K_o}} \tag{4}$$

where $K_g = nP$, $K_o = K_{oAtm} + m(P - P_{Atm})$ and $V_o = V_{oAtm}(1 + \frac{m}{K_o}(P - P_{Atm}))^{-\frac{1}{m}}$. The symbol n denotes the polytropic index of air, and for adiabatic compression and isothermal compression $n = 1$ and 1.4, respectively [16]. It is obvious that updating the volume of gas is the key step to determine the effective bulk modulus of oil.

B. THE CHANGE OF SINGLE BUBBLE IN COMPRESSED OIL

Increasing oil pressure causes the size reduction of suspended bubble in two aspects. Firstly, the bubble rapidly shrinks with the increase of pressure. At the same time, according to the Henry's law, the bubble will be continuously dissolved or released in the oil until saturation [23], [24]. The mass transfer velocity between bubble and oil is the key factor to calculate the volume of air during the compression.

Eq. (5) describes the mass flux of the entrained air diffused into the liquid [14].

$$\dot{m_g} = -K_m \xi (W_{gE} - W_g) \tag{5}$$

where, the mass transfer coefficient $K_m = \varepsilon \sqrt{\Delta P \rho_g}$, and ΔP denotes the difference between the bubble pressure and atmospheric pressure. The symbol ξ is the surface area bewteen the bubble and the oil. The dimensionless constant ε is defined as

the mass transfer scalar and determined to be 1.3×10^{-6} by experiment.

With Eq. (5), the differential equation of bubble volume changes with time is defined as follows.

$$(V_b \rho_g)' = -K_m S_b \left(W_{gS} - W_g\right) \tag{6}$$

where,

$$V_b = \frac{4}{3}\pi(\frac{d}{2})^3 \tag{7}$$

$$S_b = \pi d^2 \tag{8}$$

$$\rho_g = \rho_{gAtm}\frac{273}{273+T}\cdot\frac{P}{P_{Atm}} \tag{9}$$

The air Bunsen solubility of oil [25] is given as follows.

$$\delta = 0.116\frac{P}{P_{Atm}} \tag{10}$$

According to Eq. (10), the saturated solubility of oil can be obtained as follows.

$$W_{gS} = \frac{\delta\rho_{gAtm}}{\delta\rho_{gAtm} + \rho_l} \tag{11}$$

Substituting Eqs. (7)∼(11) into Eq. (6), the differential equation of bubble diameter can be obtained.

$$\dot{d} = -\frac{(273+T)\,2P_{Atm}K_m}{273\rho_{gAtm}P}\left(W_{gS} - W_g\right) - \frac{d}{3P}\dot{P} \tag{12}$$

where, the first term on the right side of Eq. (12) is caused by dissolution, and the second term is caused by the pressure change rate. Eq. (12) incorporates the effect of variable pressure on bubbles with changing size, and can be further used to calculate the change of bubble diameter under variable pressure conditions.

C. THE CHANGE OF AIR CONTENT IN STATIC COMPRESSED OIL

1) THE BULK MODULUS MODEL OF STATIC OIL WITH AVERAGE DIAMETER (MODEL A)

The change of air content α and the mass of residual free air m_g can be obtained by extending the dissolution and compression of single bubble to the whole oil as follows.

$$\alpha = \alpha_{Atm}\frac{V_b}{V_{init}} = \alpha_{Atm}\left(\frac{d}{d_{init}}\right)^3 \tag{13}$$

$$m_g = \rho_g\alpha = \rho_g\alpha_{Atm}\frac{d^3}{d_{init}^3} \tag{14}$$

where, d is represented the average diameter of the suspended bubble in oil.

For simplicity, all calculations are based on oil per unit volume in this paper. During the manufacturing, transporting and storing of hydraulic oil, the oil has adequate time to contact with air until reaching saturation. we assume the solution of air in oil at atmospheric pressure has reached saturation. Therefore,

$$W_g = \frac{m_{gAtm} - m_g + m_{gsAtm}}{m_l + m_{gAtm} + m_{gsAtm}} \tag{15}$$

The change of bubble size in the oil can be obtained by combining Eqs. (12), (14) and (15). However, it is a challenge to determine d by the traditional method since Eq. (12) is a complex nonlinear differential equation. To address this issue, this paper will employ the piecewise linearization method and the linear parameter variable (LPV) model to determine d. The flow diagram of Model A is shown in figure1.

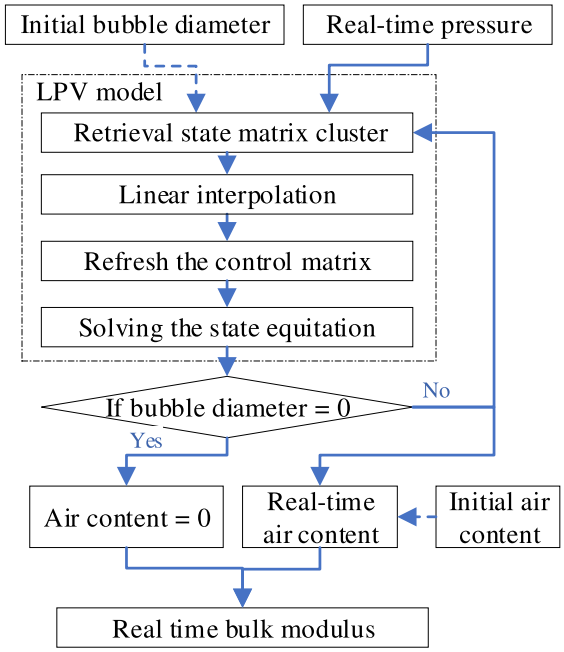

FIGURE 1. The flow diagram of Model A.

Eq. (12) can be defined in the state space form as follows:

$$\dot{d} = Ad + Bu \tag{16}$$

where,

$$\begin{cases} A = 0 \\ B = \left[-\dfrac{(273+T)}{273}\dfrac{2P_{Atm}K_m}{\rho_{gAtm}P}(W_{gS} - W_g) \quad -\dfrac{d}{3P}\right] \\ u = \begin{bmatrix} 1 \\ \dot{P} \end{bmatrix} \end{cases}$$

The control matrix B, a time-varying matrix, changes with the bubble diameter d and the system pressure P dynamically.

Within a certain range, d and P are discretized to pairs for calculating the state space matrix cluster about B. In each step of the calculation, the program would retrieve the state space cluster with the real-time P and the previous step result d. Then the ideal state matrix B for the calculation of next step is obtained by linear interpolation among the retrieved matrices which are closest to the retrieval demand. Finally, the nonlinear differential equation can be approximately solved by a linear state equation in an extremely short period. Figure 2 is the LPV model in the Simulink® environment.

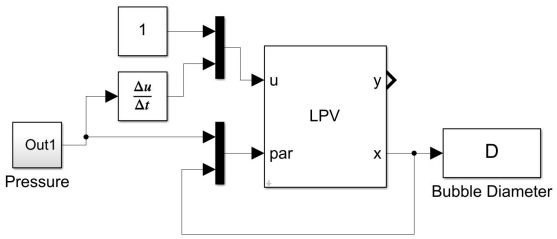

FIGURE 2. The LPV Model in the Simulink® environment.

2) THE BULK MODULUS MODEL OF STATIC OIL WITH DISTRIBUTION DIAMETER(MODEL B)

In reality, bubbles in the oil are not uniform in size. Their size corresponds to the different mass transfer rates. Therefore, calculating the bulk modulus of oil with the average diameter will result in an inaccurate outcome.

It is of great importance to understand the distribution of bubble size in oil. Gaillard *et al.* [26] pointed out the bubble size distribution depends little on the foaming device and the gas fraction, and even the bubble age does not play an important role in changing the initial distribution. However, the change of the liquid viscosity contributes to the varying of the distribution parameters of the bubble size. Although the hydraulic oil has different grades, its viscosity values are very close. Therefore, the bubble microscope photo published by literature [14] represents the general law that reflects the distribution of bubble size, and can be used to estimate the distribution style and parameters of bubble size in the hydraulic oil.

The bubble diameter in the image is measured and counted by employing image processing technology as shows in figure 3.

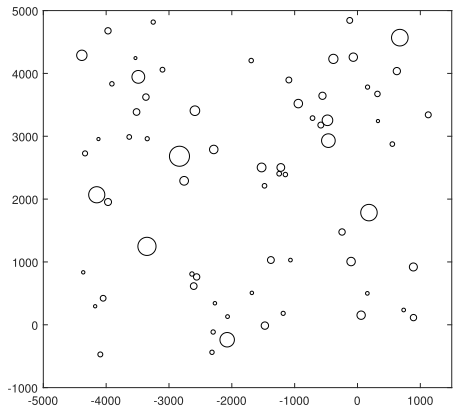

FIGURE 3. The processed results of the bubble microscopic image in the literature [14].

The statistic theory is primarily used for the purpose of obtaining the distribution of bubble size. Assuming the sample of the bubble diameter follows a log-normal distribution, its distribution parameters can be estimated by the method of maximum likelihood. The estimated results indicate the radius of bubble in oil follows the distribution of $\ln(X) \sim N(3.9, 0.47^2)$. At the same time, the χ^2 test is conducted on the hypothesis of the bubbles' size obeying the log-normal distribution. The results show the χ^2 goodness-of-fit test does not reject the null hypothesis at the significance level of 0.5%. Therefore, the null hypothesis can be safely rejected, and we can conclude that the radius of bubble in the hydraulic oil are subjected to the log-normal distribution.

The Literature [14] pointed out that on the premise that the bubble radius is less than 130um, it only takes about 0.1s to compress the bubble to temperature equilibrium. According to the log-normal distribution of bubble size, the proportion of bubbles with the radius greater than 130um is less than 1%. We can assume that the bubble size in the oil is in the range of 0-130um, and the compression can be assumed to be an isothermal process.

In order to well understand the effect of dissolution rate on the bulk modulus, the oil is equally divided into k segments after all bubbles are removed. At the same time, all bubbles are divided into k segments based on bubble size. The remixing of bubbles and oil is shown in figure 4. Each layer of the liquid can be assumed as a spring. The density of bubble number in each layer determines the air content and stiffness, the average diameter of each layer affects the dissolution rate caused by time and pressure. Thus, the air content α_{Atm} can be determined as follows.

$$\alpha_{Atm} = \sum_{i=1}^{k} \frac{4}{3}\pi \left(\frac{d_i}{2}\right)^3 N \cdot rate_i \tag{17}$$

where N denotes the total number of bubbles, d_i is the average diameter of bubbles in layer i, $rate_i$ is the cumulative probability of bubbles in layer i. N can be determined by (17). The dynamic air content of each layer can be calculated by Model A. Finally, the air content of the whole oil can be obtained by the sum of the air volume of k layers. The flow diagram of Model B is pictured in figure 5.

D. THE EFFECTIVE BULK MODULUS MODEL OF FLOWING OIL (MODEL C)

The oil compressed by the pump in the hydraulic pipeline maintains the one-way movement on the way to the actuator or the commutator. To estimate the effective bulk modulus of flowing oil in the pipeline, the flowing oil is equivalent to the model in figure 6, where L is the length of the pipeline, dl is the infinitesimal length of oil at position l, and the bulk modulus of dl is denoted by K_l.

Neglecting the effect of system leakage and liquid compression deformation on the flow, the dl compression time t_l and the system flow $q(t)$ satisfy the flow balance equation as follows.

$$lS_{pipe} = \int_0^{t_l} q(t)dt \tag{18}$$

According to the definition of bulk modulus, the effective bulk modulus of the whole oil K_{pipe} and the infinitesimal K_l

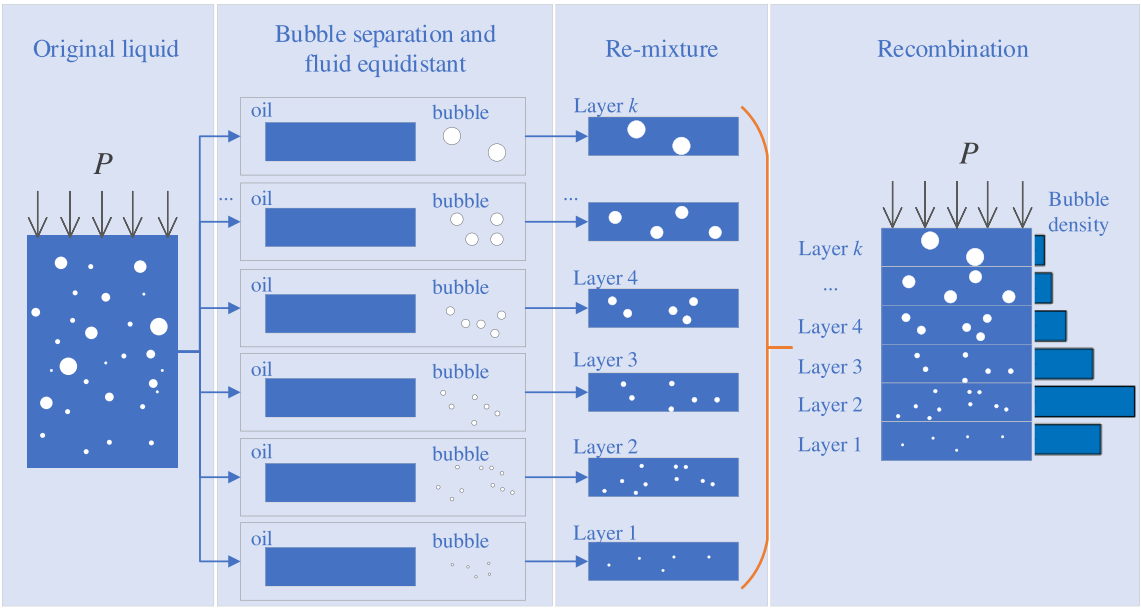

FIGURE 4. The schematic of Model B.

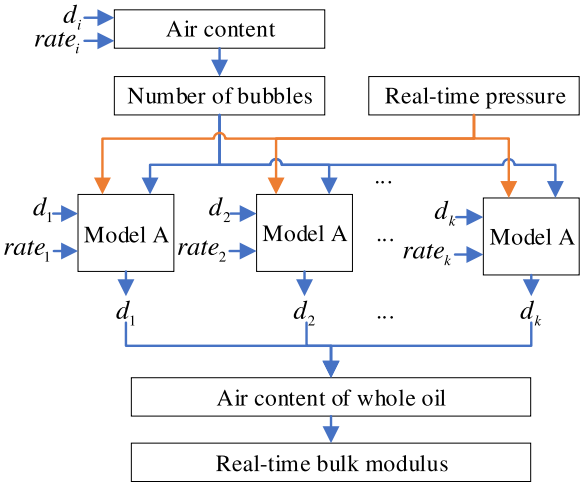

FIGURE 5. The flow diagram of Model B.

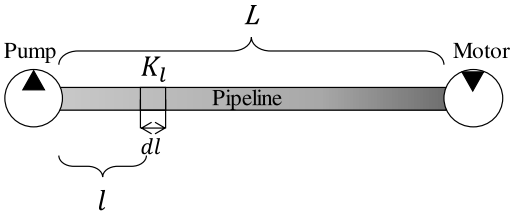

FIGURE 6. The flowing oil Model.

are expressed in Eq. (19) and Eq. (20), respectively.

$$K_{pipe} = -\frac{dP}{dV} = LS_{pipe}\frac{dP}{\int_0^L dV_{dl}} \tag{19}$$

$$K_l = -dlS_{pipe}\frac{dP}{dV_{dl}} \tag{20}$$

where, dV_{dl} is the infinitesimal of liquid volume change.

Assuming the pipeline is rigid, the deformation of oil caused by compression only occurs in the flow direction. Substituting Eq. (20) into Eq. (19) leads to the following equation.

$$K_{pipe} = L\frac{dP}{\int_0^L \frac{dP}{K_l}dl} = L\frac{1}{\int_0^L \frac{1}{K_l}} \tag{21}$$

Ignoring the oil compression time in the pump and the pressure loss in the pipeline, K_l is determined by substituting the system pressure $P(t)$ into Model B. It is worth noting that the mass transfer scalar could be approximately employed only if the flow is laminar. Therefore, before using the above method to calculate the equivalent bulk modulus of flowing oil, the Reynolds criterion is specifically used to determine the flow state of the oil.

$$R_e = \frac{QD}{vS_{pipe}} \tag{22}$$

where, R_e denotes the Reynolds number, Q is the flow, D is the diameter of the pipeline, and v is the viscosity of the oil.

III. EXPERIMENTAL VERIFICATION

A. THE BULK MODULUS OF THE STATIC HYDRAULIC OIL IN VESSEL

1) TEST INTRODUCTION

Based on the volume change method, Gholizadeh *et al.* [16] designed a test bench with controllable air content to measure the bulk modulus of static oil. During the experiment, bubbles of different sizes were injected into the oil by the venturi orifice. The bulk modulus of the static oil was calculated by measuring the changes in vessel volume and the oil pressure. They conducted a series of tests under variable pressure conditions and published the details of system pressure and bulk

modulus changing over time. The bulk modulus of the pure oil under atmospheric pressure is 1970 MPa, and the slope of the oil bulk modulus versus pressure curve $m = 5.6$. Those experiment results will be introduced to verify Model A and Model B in this paper.

2) VERIFICATION OF MODEL A AND MODEL B

The load spectra of the aforementioned experiments are input into Model A and Model B respectively for computing the development of the oil bulk modulus. The test and the simulation results are compared in figure 7 and figure 8, where the figure within a figure is the load spectra of the test.

Figure 7 and figure 8 are the experimental and the simulation results of static oil bulk modulus at the operating temperature $24 \pm 1°C$. It can be found that the oil bulk modulus raised rapidly with the increase of the pressure, and the volume compression rate or loading rate also affect the value of bulk modulus.

Figure 7 depicts the experimental and theoretical bulk modulus values as a function of pressure for $\alpha_{Atm} = 1.5\%$, 3.35% and 4.5% under the rapid volume change rate. Figure 8 depicts the experimental and theoretical bulk modulus values as a function of pressure for 3.45% and 4.4% under intermediate volume change rate. The results indicate both Model A and Model B can well-reproduce the test results, and the volume change rate and the initial air content have crucial effect on the bulk modulus of the static oil. However, the simulation results of Model B, which considers the distribution of bubble size, are closer to the experimental results.

B. THE BULK MODULUS OF THE FLOWING OIL IN THE PIPELINE

1) EXPERIMENT PRINCIPLE

The authors [16], [22], [27], [28] have measured the bulk modulus of oil in a variety of ways. However, there are only a few methods related to the bulk modulus of the oil in the pipeline. Xiaole and Lichen [24] realized the online measurement of the oil bulk modulus by identifying the natural frequency of the oil. Cho *et al.* [29] calculated the bulk modulus by measuring the transfer velocity of pressure wave, which generated by opening or closing the solenoid valve. However, those methods are either easily disturbed by the environment or interfered with the flow and the pressure of the system. To deal with those issues, the operating principle of the axial piston pump has attracted our attention.

During the operation of the axial piston pump, when the plungers is moved from the low-pressure chamber to the high-pressure chamber, the pressure will fluctuate periodically due to the backflow of oil and other reasons. It should be noted the velocity of fluctuation which spreading in pipeline reflects the compressibility of the flowing oil. Therefore, the pressure pulsation of the axial piston pump can be employed as an excitation signal to measure the transfer velocity of the pressure pulsation in pipeline.

The transmission time of the pressure pulsation could be obtained by calculating the cross-correlation of the

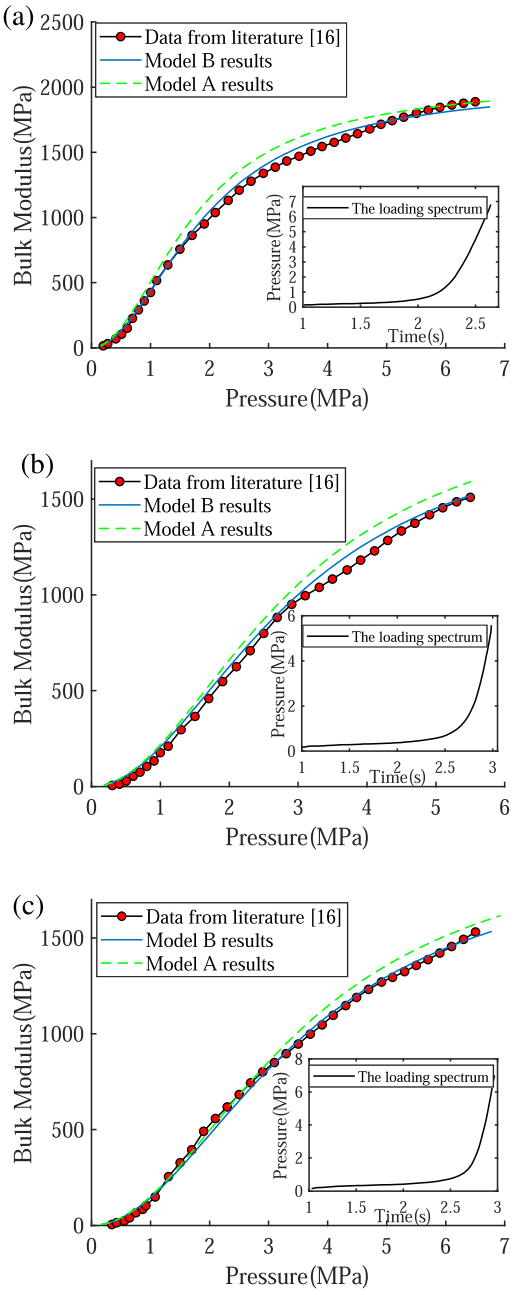

FIGURE 7. The experimental and simulation results of different air content under the rapid volume change rate. (a) $\alpha_{Atm} = 1.5\%$, (b) $\alpha_{Atm} = 3.35\%$, (c) $\alpha_{Atm} = 4.5\%$.

synchronization pressure signals obtained from the measuring points. Compared to the velocity of the pressure pulsation, the velocity of the flow can be neglected. With the above information, the bulk modulus of flowing oil can be calculated by Eq. (23) [30].

$$K_{pipe} = \rho_l \left(\frac{L}{t}\right)^2 \tag{23}$$

where, t denotes the transmission time of the pressure pulsation between measuring points.

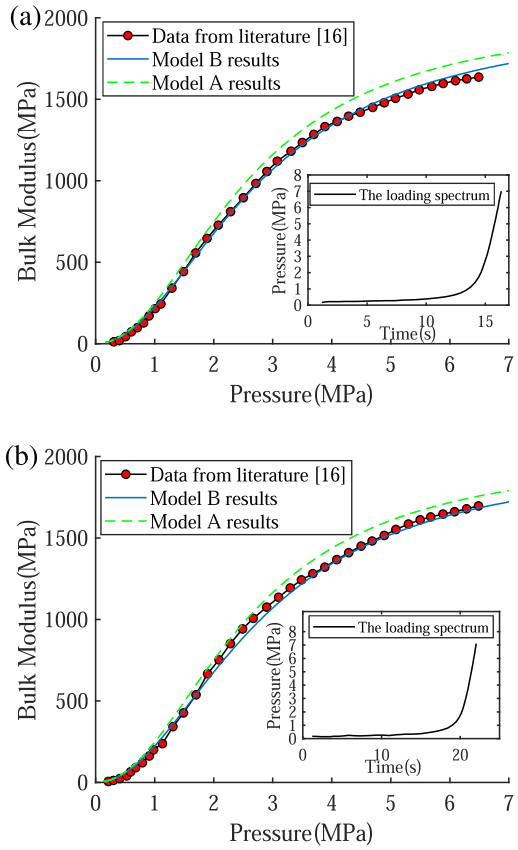

FIGURE 8. The experimental and simulation results of different air content under the intermediate volume change rate. (a) $\alpha_{Atm} = 3.45\%$, (b) $\alpha_{Atm} = 4.4\%$.

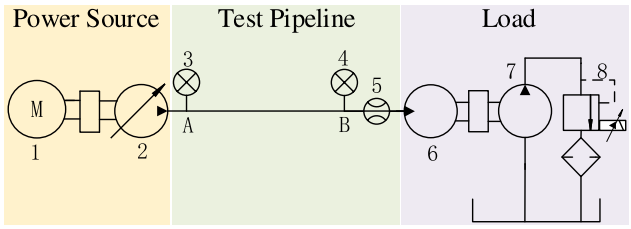

FIGURE 9. The schematic diagram of the experimental hydraulic system circuit: 1 Inverter-fed motor, 2 Variable displacement axial piston pump, 3 and 4 Pressure transmitter, 5 Flow meter, 6 Hydraulic motor, 7 Gear pump, 8 Proportional relief valve.

In fact, ρ_l is the density of the liquid mixed with bubbles. However, the dissolution of the bubble, especially the compression of bubbles, contributes to the approximate value of the pure oil density and the liquid density. To simplify the calculations, it is assumed the density of fluid equals to the pure oil when the pressure is over 2MPa.

2) EXPERIMENTAL DESIGN

The schematic diagram of the test bench is shown in figure 9 and the main technical parameters of key components are illustrated in table 1. The test bench is a pump-controlled variable frequency and variable displacement compound speed regulating hydraulic system. The variable displacement axial piston pump 2 driven by the inverter-fed motor 1 is the hydraulic power source. The controllable load condition is conducted by the relief valve 8 and motor 6. Changing the working pressure of the relief valve 8 could change the load torque of the hydraulic motor 6, thereby changing the oil pressure in the pipeline. The flow meter 5 is employed to measure the flow of the pipeline. The flow can be changed by changing the rotation speed of the inverter-fed motor 1 or the displacement of the axial piston pump 2.

TABLE 1. Main technical parameters of key components.

Key component	Technical parameter	Content
Inverter-fed motor	Type	Siemens 1LG0206-4AA70-Z
	Rated power	30KW
	Rated speed	1470r/min
Variable displacement axial piston pump	Type	HPV55-02RE1X300E
	displacement	0-55ml
	Rated pressure	42 MPa
	Maximum speed	3300 r/min
Hydraulic motor	Type	HMV105-02E1C
	displacement	35-105 ml
	Rated pressure	42 MPa
	Maximum speed	3500 r/min
Gear pump	Type	CBY4150-A3Fl
	displacement	50ml
	Rated pressure	20Mpa
	Maximum speed	2000 r/min

To measure the transfer velocity of the pulsation in the pipeline, a pair of oil pressure transmitters 3 and 4 are installed at the pump outlet A and the specified position B of rigid tubing respectively.

During the data acquisition, the inverter will cause power frequency interference in the electrical signal of the sensors. In response to this issue, the photoelectric isolation protection is adopted to protect the pressure signal of two channels during the measurement to resist the interference of power frequency. At the same time, the NI industrial computer that matches NI PXI-6122 synchronous data acquisition card is designed to ensure the synchronicity and stability of the pressure data of the pressure transmitters 3 and 4.

The high-frequency noise leads to the difficulty in identifying the peak value of the cross-correlation results of pressure signal. Although hardware has been equipped to make the signal as clear as possible, it still cannot completely avoid high-frequency noise being mixed into the collected signals. Therefore, the measured signal must be further filtered. To ensure that there is no phase lag in the filtering of high-frequency noise, zero-phase distortion digital filtering technology is adopted. Figure10 is the flow diagram of the online measurement of oil bulk modulus.

3) MODEL VERIFICATION

The distance between pressure transmitter 3 and 4 is 2.2m, the inner diameter of the pipe is 2cm, and the oil grade is

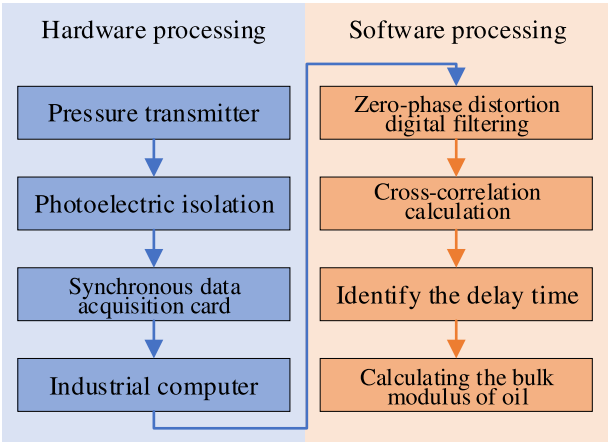

FIGURE 10. The flow diagram of the oil bulk modulus online measurement.

L-HL46. According to the Reynolds criterion, as long as the flow is less than 678L/min, the flow in the pipeline can be regarded as the laminar flow. During operation, the pipeline temperature is maintained at $30 \pm 1°C$ by the cooling fan.

The major drawback of this experiment is that the air content of the oil in the pipeline cannot be measured. However, it is certain that the air content of the oil at atmospheric pressure does not change during the continuous operation of the system. Therefore, one set of experimental results is used to estimate the air content with Model C firstly. Then the estimated air content is used to predict other results. If all experiment curves and simulation curves are well-fitted, it means Model C is valid.

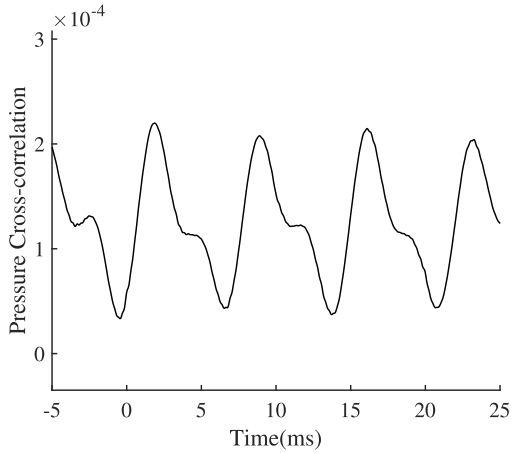

FIGURE 11. A cross-correlation function of the pressure signals.

Figure11 illustrates a set of cross-correlation results of the pressure signals. The periodic waveform in figure11 is caused by the periodic pressure pulsation of the axial piston pump. During the operation, the pressure pulsation of measuring point B always lags behind measuring point A. Therefore, in the cross-correlation curve of the pressure

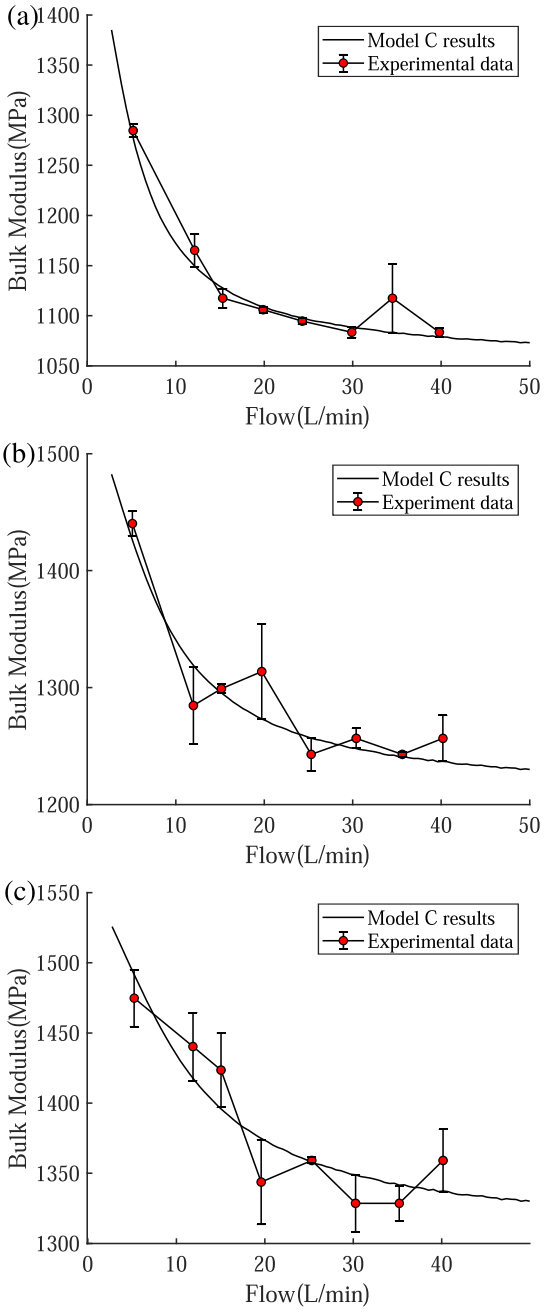

FIGURE 12. The experimental and simulation results of the flowing oil bulk modulus. (a) $P = 6$MPa, $\alpha_{Atm} = 2.9\%$ estimated by Model C, (b) $P = 8$MPa, $\alpha_{Atm} = 2.9\%$ (c) $P = 10$MPa, $\alpha_{Atm} = 2.9\%$.

signals B and A, the first wave peak on the right side of the 0 scales is the transmitting time of pressure wave.

By measuring the delay time of pressure pulsation between the measurement points under different flow and pressures, the bulk modulus of the oil in different operation conditions can be calculated according to Eq. (23). Figure 12 shows the flowing oil bulk modulus of Model C and the tested results.

When the system pressure is 6MPa, the simulated air content is set to 2.9%, the curves of simulation to experiment are fitted well in figure12(a). Then maintaining the simulation

air content and changing the simulation pressure to 8MPa and 10MPa, Model C results are also in good agreement with the experimental data under 8MPa and 10MPa, respectively, shown in figure12(b)and(c). Thus, the experiment results illustrate the feasibility of using Model C to predicting the bulk modulus of flowing oil.

The most interesting finding from the simulation and experimental results is that when the hydraulic system is operated at low-flow condition, the equivalent bulk modulus of the flowing oil is large. As the flow increases, the bulk modulus of the oil decreases rapidly. When the flow reaches a certain level, the equivalent bulk modulus tends to be stable, which can be approximated as invariant. The bulk modulus of oil exhibits strong nonlinear characteristics of flow function. This phenomenon can be explained as follows. With the increase of the flow rate, the replacement of the oil in the pipeline becomes faster. Thus, there is less time for bubbles to be dissolved into the oil. The less dissolution time contributes to a decrease in the bulk modulus.

IV. EXPANDING RESEARCH

A. EXPANDING RESEARCH OF MODEL A AND MODEL B

During the compression, the real-time air content of the static oil is determined by the compression process and the initial bubble size. In this section, the effects of the bubble size and loading rate on the bulk modulus of static oil are analyzed. The simulation temperature and the air content are 24 °C and 3%, respectively. The bulk modulus of pure hydraulic oil is 1510 MPa at atmospheric pressure, m=5.6. The effect of the bubble size and compression rate on the oil bulk modulus is quantitatively analyzed using Model A and Model B, respectively.

1) EFFECT OF BUBBLE SIZE ON BULK MODULUS

Model A is used to analyze the bulk modulus of oil with bubbles of different average diameters. For more intuitive comparison, all curves of the air content are the air content at atmospheric pressure in this paper.

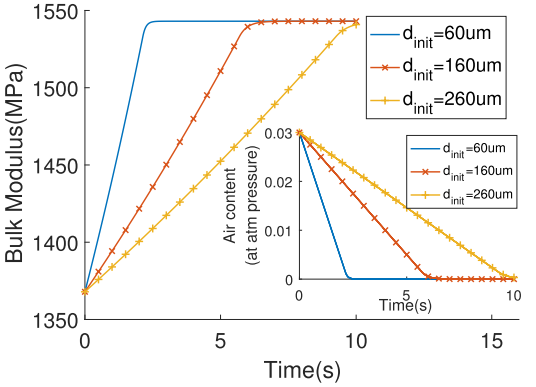

FIGURE 13. Effect of different bubble diameters on the oil bulk modulus.

The figure within the figure13 is the real-time air content of the compression oil. The figure13 shows that the change rate of the bulk modulus corresponds to the change rate of the real time air content. Under the same condition of the air content 3% and the system pressure 6 MPa, the larger the bubble size, the slower the air dissolves. This conclusion can be explained as, with the increase of the average bubble size, the contact surface between the bubbles and the oil becomes smaller. The slowly dissolved bubble results in the sluggish increase of the bulk modulus. The conclusion also proves that the bubble diameter has a great effect on the determination of the oil bulk modulus. It is necessary to consider the bubble size distribution for accurate calculation of the oil bulk modulus.

2) EFFECT OF THE BUBBLE SIZE DISTRIBUTION ON THE BULK MODULUS

We equally divided the liquid into 6 segments after all bubbles are removed (as show in figure 4). At the same time, all bubbles are divided into 6 segments on bubble size. Then, remixing the bubbles and the oil. Figure 14 shows the simulation results of the bulk modulus with an air content of 3% and a bulk modulus of 1510 MPa at atmospheric pressure. The oil pressure varies from 0.1 MPa to 10.1MPa at the rate of 1 MPa/s. The loading spectrum has been illustrated in figure 14(a).

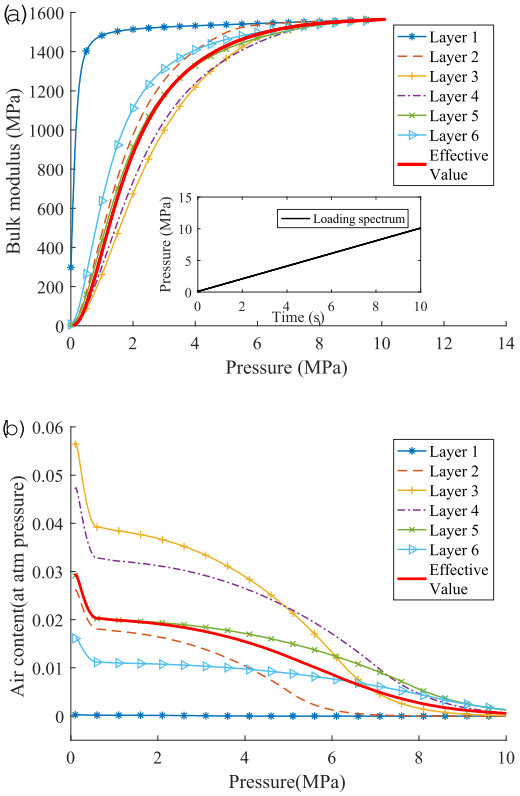

FIGURE 14. Effect of bubble size distribution on bulk modulus under the same pressure. (a) The bulk modulus, (b) The air content.

The distribution of bubble size can be considered as weight of different bubble dissolution rates in total dissolution rate. According to the log-normal distribution (bubble density in figure 4), although the number of bubbles in layer 2 is

the largest, the total air content of the layer 3, layer 4 and layer 5 exceed the second layer, which caused by the different bubble diameter of each layer. The shrinking rate of bubble caused by the pressure in each layer of liquid is consistent. However, the average bubble diameter of each layer contributes to the different bubble dissolution rates. It affects the real-time air content of each layer, thus affects the change of the effective bulk modulus of whole liquid.

3) EFFECT OF THE LOADING RATE ON THE BULK MODULUS

The bulk modulus of the static oil with different loading rates is calculated by Model B. In figure15, the oil pressure varies from 0.1 MPa to 9.1 MPa at the rate of 1MPa/s, 1.5MPa/s, and 3MPa/s, respectively. The change of the bulk modulus and the air content are illustrated in figure 15.

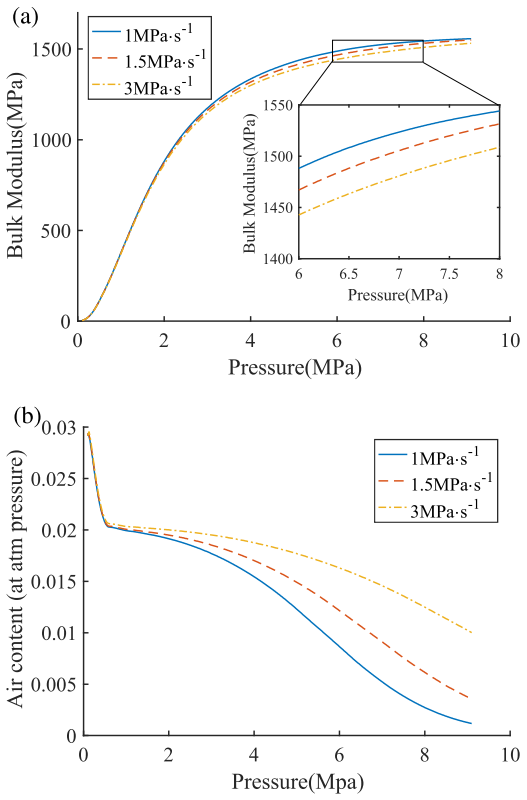

FIGURE 15. Effect of different bubble diameters on bulk modulus under the same pressure. (a) The bulk modulus, (b) The air content.

Figure15(b) shows, in the range of 0.1∼1 MPa, the air dissolution is mainly determined by the system pressure, and the effect of different compression rates on the dissolution can be neglected. After 1MPa, the compression rate becomes the main factor affecting the air dissolution. As the system pressure increases, the bubble diameter in the oil decreases under the dual effects of compression and dissolution. When the gas content drops to 0.5%, the decrease of the bubble diameter results in the shrink in the contact area between the oil and the bubbles, which responsible for slowing down the dissolution rate.

After 2 MPa, the cumulative difference of the air content caused by the compression rate brings in a significant difference of effective bulk modulus in Figure15(a). When the pressure reaches 8 MPa, the cumulative difference of air content among the different compression rate curves reach the maximum. With the further dissolution of the bubble and the further increase of the pressure, the bulk modulus of the oil equals that of pure oil, in the end. This is consistent with previous research conclusions.

According to the above analysis, the dissolution rate of the bubbles under variable operation condition is determined by bubble diameter, system pressure, and compression rate. The whole compression process presents non-linear characteristics.

B. EXPANDING RESEARCH OF MODEL C

By Model C, the effect of pressure, air content, pipeline size, and flow on the bulk modulus of the flowing oil is quantitatively discussed in the following paragraphs.

The simulation parameters of Model C are set as follows. The bulk modulus of pure oil is 1510MPa, m=5.6, the dynamic viscosity is 360 $\times$ 10^{-6}m^2/s, the density of oil is 860kg/m^3, the simulation temperature is 30°C, and the air content is 3% at atmospheric pressure. According to the Reynolds criterion, when the inner diameter of the pipeline is less than 4 cm, as long as the flow is less than 339L/min, the oil can be regarded as a laminar flow.

Figure16 illustrates the effect of pressure, diameter and pipeline length on the equivalent bulk modulus of flowing oil, respectively. The curves of bulk modulus become flatter in response to the increase of pressure (figure 16 (a)), diameter(figure 16 (b)) and length(figure 16 (c)) of the pipeline. The results indicates the pressure is the dominated factor to affect the bulk modulus of flowing oil as in static oil. The equivalent bulk modulus of flowing oil changes a lot under the low-pressure operation condition, especially in the low-flow area. The size of the pipeline has significant effect on the bulk modulus of oil. Figure17 clarifies the relationship among bulk modulus, flow, and pressure under steady working conditions, where the air content of oil is 1%, 3% and 5%, respectively.

It is found that the higher the pressure, the smaller effect of the air content and the flow on the equivalent bulk modulus of oil in pipeline. When the pressure is high enough, the equivalent bulk modulus of liquid can be approximated to the bulk modulus of pure oil. Under the condition of the low-flow and low-pressure, the equivalent bulk modulus of oil in the pipeline is greatly affected by the air content and the flowing velocity. The equivalent bulk modulus of oil in the pipeline changes obviously with the increase of the flow under the low-flow range. By analyzing the aforementioned graphical features, some conclusions are proposed:

- The experimental and simulation results indicate that, when the air content of the oil is constant at atmospheric pressure, simply assume the bulk modulus of oil in

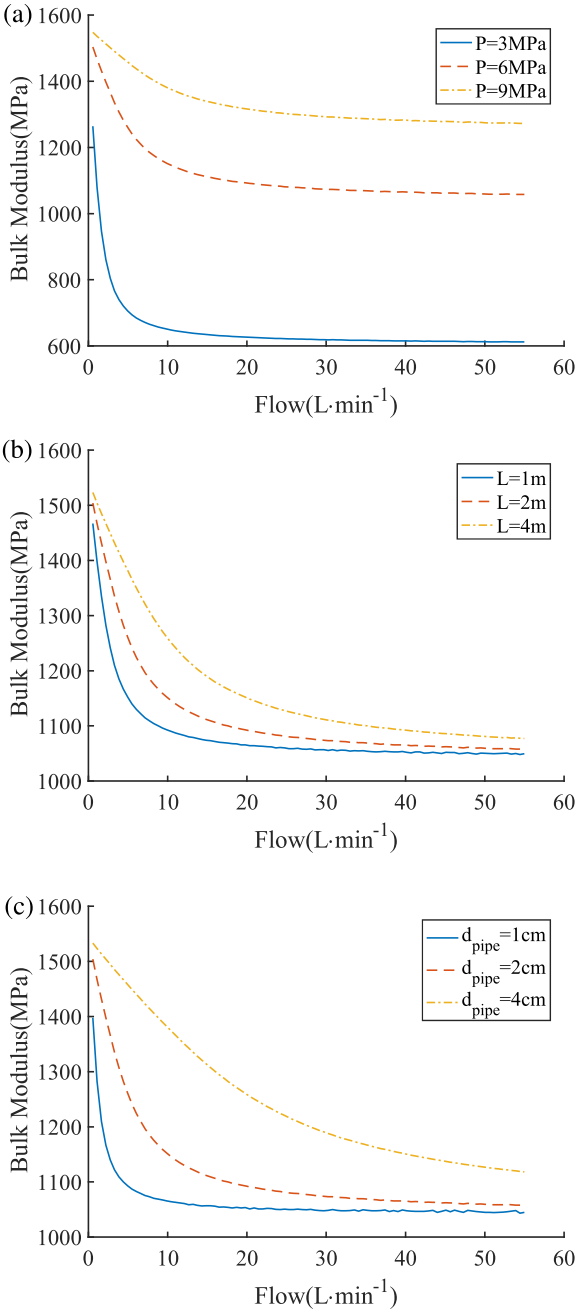

FIGURE 16. The bulk modulus of the flowing oil. (a) The bulk modulus of flowing oil under the different pressures, where, $\alpha_{Atm} = 3\%$, $L = 2$m, $d_{pipe} = 2$cm, (b) The bulk modulus of flowing oil with the different diameters of the pipeline, where, $\alpha_{Atm} = 3\%$, $P = 6$MPa, $L = 2$m, (c) The bulk modulus of flowing oil with the different lengths of the pipeline, where, $\alpha_{Atm} = 3\%$, $P = 6$MPa, $d_{pipe} = 2$cm.

pipeline as a constant or only pressure-dependent will cause errors, especially in low-flow and low-pressure operation condition.

- According to the work requirements, reasonable design of the pipeline size and control of the flowing velocity can avoid the system working in a nonlinear range of oil bulk modulus and keep the bulk modulus stable over a wider flow range.

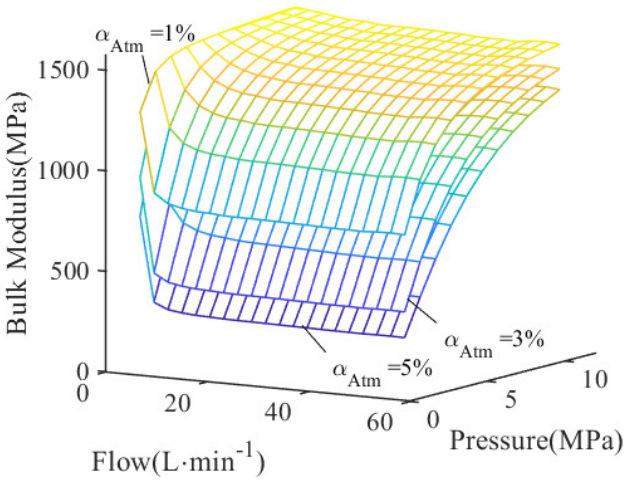

FIGURE 17. The relation among K_{pipe}, flow and pressure in different air contents.

V. CONCLUSION

The purpose of this study was to calculate and verify the bulk modulus of flowing oil. In this work, combining with the distribution of bubble size in the oil, we analyzed the compressibility of static oil under variable operation condition, and proposed an original model of the equivalent bulk modulus of flowing oil. At the same time, an innovative online measurement method for the bulk modulus of flowing oil was introduced. The strong relationship between pressure, bubble size, and flow to the oil bulk modulus have been verified and reported. The proposed flowing oil model fills the gap in determining the flowing oil effective bulk modulus. Model B and Model C are practical for system assisted design and accurate control. And both of the models can be used to study the stiffness, and the dynamic and nonlinear performance of the hydraulic system.

Restricted by the experimental conditions, only flow in the form of laminar is analyzed. However, for hydraulic pipelines containing various valves, the flow state of oil becomes more complicated, and the model proposed in this paper is ineffective. This remains to be verified by further research.

NOMENCLATURE

d = Bubble diameter, m
d_{init} = Bubble diameter at atmospheric pressure, m
K_{oAtm} = Bulk modulus of the pure oil at atmospheric pressure, MPa
K_e = Bulk modulus of the oil mixed with air, MPa
K_o = Bulk modulus of the pure oil, MPa
K_g = Bulk modulus of the air, MPa
K_m = Mass transfer coefficient from air to oil, kg/m$^2\cdot$ s
K_{pipe} = Bulk modulus of the oil in the pipeline, MPa
m = Slope of the pure oil bulk modulus versus pressure curve
m_g = mass of the free air in the oil, kg m_{gAtm} = Mass of bubbles in the oil at atmospheric, kg

m_{gsAtm} = Equilibrium mass of the air in the oil at atmospheric pressure, kg
m_l = Total mass of the oil mixed with air, kg
n = Polytropic index of the air
P = Pressure, MPa
P_{Atm} = Atmospheric pressure, MPa
S = Surface area of the bubble, m^2
T = Temperature, °C
V = Volume of the bubble, m^3
W_g = Mass fraction of the air in the liquid, kg
W_{gs} = Equilibrium mass fraction of the air in the oil at pressure p
V_g = Volume of the air in oil, m^3
V_l = Volume of the pure oil, m^3
α = Air content of the oil at pressure p, %
α_{Atm} = Air content of the oil at atmospheric pressure, %
ξ = Mass transfer scalar from the air to the oil
δ = Bunsen coefficient of the air in oil
ε = Surface area between the air and oil, m^2
ρ_g = Density of the air, kg/m^3
ρ_l = Density of the oil, kg/m^3
ρ_{Atm} = Density of the air at atmospheric pressure, kg/m^3

REFERENCES

[1] L. Gu and B. Yang, "A cooperation analysis method using internal and external features for mechanical and electro-hydraulic system," *IEEE Access*, vol. 7, pp. 10491–10504, 2019.
[2] H. Feng, Q. Du, Y. Huang, and Y. Chi, "Modeling study on stiffness characteristics of hydraulic cylinder under multi-factors," *Stroj. Vest. J. Mech. Eng.*, vol. 63, nos. 7–8, p. 447, Jul. 2017.
[3] T.-H. Wu and C.-C. Lan, "A wide-range variable stiffness mechanism for semi-active vibration systems," *J. Sound Vib.*, vol. 363, pp. 18–32, Feb. 2016.
[4] Y. Gao, Y. Shen, T. Xu, W. Zhang, and L. Guvenc, "Oscillatory yaw motion control for hydraulic power steering articulated vehicles considering the influence of varying bulk modulus," *IEEE Trans. Control Syst. Technol.*, vol. 27, no. 3, pp. 1284–1292, May 2019.
[5] B. Yu, R. Liu, Q. Zhu, Z. Huang, Z. Jin, and X. Wang, "High-accuracy force control with nonlinear feedforward compensation for a hydraulic drive unit," *IEEE Access*, vol. 7, pp. 101063–101072, 2019.
[6] J. Wang, G. Gong, and H. Yang, "Control of bulk modulus of oil in hydraulic systems," in *Proc. IEEE/ASME Int. Conf. Adv. Intell. Mechatronics*, Jul. 2008, pp. 1390–1395.
[7] Y. Zhao, G. Chen, C. Miao, and C. Zhang, "Design and dynamic performance analysis of an electro-hydraulic robot joint," in *Proc. 3rd Int. Conf. Mech., Control Comput. Eng. (ICMCCE)*, Sep. 2018, pp. 251–257.
[8] W. Shen, H. Huang, Y. Pang, and X. Su, "Review of the energy saving hydraulic system based on common pressure rail," *IEEE Access*, vol. 5, pp. 655–669, 2017.
[9] J. Yao, Z. Jiao, D. Ma, and L. Yan, "High-accuracy tracking control of hydraulic rotary actuators with modeling uncertainties," *IEEE/ASME Trans. Mechatronics*, vol. 19, no. 2, pp. 633–641, Apr. 2014.
[10] S. Vasquez, M. Kinnaert, and R. Pintelon, "Active fault diagnosis on a hydraulic pitch system based on frequency-domain identification," *IEEE Trans. Control Syst. Technol.*, vol. 27, no. 2, pp. 663–678, Mar. 2019.
[11] J. Ma, "Flow ripple of axial piston pump with computational fluid dynamic simulation using compressible hydraulic oil," *Chin. J. Mech. Eng.*, vol. 23, no. 01, p. 45, 2010.
[12] Q. Tian and L. Gu, "Instantaneous speed fluctuation extraction and its application for efficiency evaluation of hydraulic system," *Austral. J. Mech. Eng.*, pp. 1–7, 2019.
[13] H. Gholizadeh, R. Burton, and G. Schoenau, "Fluid bulk modulus: A literature survey," *Int. J. Fluid Power*, vol. 12, no. 3, pp. 5–15, Jan. 2011.
[14] H. Tian and J. D. Van de Ven, "Modeling and experimental studies on the absorption of entrained gas and the influence on fluid compressibility," *J. Fluids Eng.*, vol. 139, no. 10, 2017, Art. no. 101301.
[15] K. Schmitz and H. Murrenhoff, "Modelling of the influence of entrained and dissolved air on the performance of an oil-hydraulic capacity," *Int. J. Fluid Power*, vol. 16, no. 3, pp. 175–183, Sep. 2015.
[16] H. Gholizadeh, D. Bitner, R. Burton, and G. Schoenau, "Modeling and experimental validation of the effective bulk modulus of a mixture of hydraulic oil and air," *J. Dyn. Sys., Meas., Control*, vol. 136, no. 5, 2014, Art. no. 051013.
[17] S. Sakama, Y. Tanaka, and H. Goto, "Mathematical model for bulk modulus of hydraulic oil containing air bubbles," *Mech. Eng. J.*, vol. 2, no. 6, 2015, Art. no. 150347.
[18] D. Bach, J. H. Harmening, M. Höfer, T. Masselter, and T. Speck, "Separation of entrained air bubbles from oil in the intake socket of a pump using oleophilic and oleophobic woven and nonwoven fabrics," *J. Fluids Eng.*, vol. 140, no. 3, 2018, Art. no. 031301.
[19] W. Chao, Z. Junjie, and S. Yuan, "Comparison of steady and dynamic models for the bulk modulus of hydraulic oils," *Acta Armamentarii*, vol. 36, no. 7, pp. 1153–1159, 2015.
[20] M. Rundo, R. Squarcini, and F. Furno, "Modelling of a variable displacement lubricating pump with air dissolution dynamics," *SAE Int. J. Eng.*, vol. 11, no. 2, pp. 111–126, May 2018.
[21] I. F. Furno, "Effects of air dissolution dynamics on the behaviour of positive-displacement vane pumps: A simulation approach," in *Proc. 10th Int. Fluid Power Conf. (10. IFK)*, vol. 1, Mar. 2016, pp. 361–372.
[22] J. Zhou, A. Vacca, and B. Manhartsgruber, "A novel approach for the prediction of dynamic features of air release and absorption in hydraulic oils," *J. Fluids Eng.*, vol. 135, no. 9, 2013, Art. no. 091305.
[23] S. Kim and H. Murrenhoff, "Measurement of effective bulk modulus for hydraulic oil at low pressure," *J. Fluids Eng.*, vol. 134, no. 2, 2012, Art. no. 021201.
[24] X. Yan, "Online measurement of effective bulk modulus in hydraulic system by the soft-sensing model," *J. Mech. Eng.*, vol. 47, no. 10, pp. 126–132, 2011.
[25] G. Guanzhu, F. Yurun, and J. Fengchang, "Solubility of air in dimethyl silicone and hydraulic oils," *Acta Phys. Chim. Sinica*, vol. 24, no. 7, pp. 1225–1232, 2008.
[26] T. Gaillard, M. Roché, C. Honorez, M. Jumeau, A. Balan, C. Jedrzejczyk, and W. Drenckhan, "Controlled foam generation using cyclic diphasic flows through a constriction," *Int. J. Multiphase Flow*, vol. 96, pp. 173–187, Nov. 2017.
[27] K. Schrank, H. Murrenhoff, and C. Stammen, "Investigation of different methods to measure the entrained air content in hydraulic oils," in *Proc. ASME/BATH Symp. Fluid Power Motion Control*, Nov. 2014, pp. 1–8.
[28] S. Fei and D. Kong, "Bulk modulus measurement of hydraulic oil based on drop-hammer calibration device," in *Proc. Int. Conf. Electr. Inf. Control Eng.*, Apr. 2011, pp. 213–216.
[29] B.-H. Cho, H.-W. Lee, and J.-S. Oh, "Estimation technique of air content in automatic transmission fluid by measurign effective bulk modulus," SAE Tech. Paper, Warrendale, PA, USA, Tech. Rep. 1229-9138(pISSN)/1976-3832(eISSN), 2000.
[30] Y. Jinghong, C. Zhaoneng, and L. Yuanzhang, "The variation of oil effective bulk modulus with pressure in hydraulic systems," *J. Dyn. Syst., Meas., Control*, vol. 116, no. 1, pp. 146–150, Mar. 1994.

BAOLONG GENG received the B.S. degree in mechatronics engineering from Tianjin Polytechnic University, China, in 2010, and the M.S. degree in mechatronics engineering from the Huazhong University of Science and Technology, Wuhan, China, in 2012. He is currently pursuing the Ph.D. degree with the Xi'an University of Architecture and Technology, China.

His research interests include hydraulic transmission and control, mechanical condition monitoring, and intelligent fault diagnosis.

LICHEN GU received the M.S. degree in structural mechanics from the Xi'an University of Architecture and Technology, Xi'an, China, in 1994, and the Ph.D. degree in mechatronics engineering from Xi'an Jiaotong University, Xi'an, in 2002. From 2010 to 2011, he was a Senior Visiting Scholar with the Georgia Institute of Technology, Atlanta, GA, USA. He is currently a Full Professor of mechanical engineering with the Xi'an University of Architecture and Technology and a part-time Professor with the State Engineering Laboratory of Highway Maintenance Equipment, Chang'an University, Xi'an. His research interests include dynamic measurement and fault diagnosis for hydraulic equipment, hydraulic transmission and control, and mechatronic design.

JIAMIN LIU received the B.S. degree in mechanism design, manufacturing and automatization from the Xi'an University of Architecture and Technology, Xi'an, China, in 2016, where she is currently pursuing the Ph.D. degree in mechanical design and theory.

Her research interests include condition monitoring and fault detection of mechanical electro-hydraulic systems.